Basic Machine Parameters

- Number of Blades: 2
- Rotor diameter: 10.058 m or 11.064 m with tip extension
- Hub height: 12.192 m
- Type of rotor: teetered or rigid
- Rotational speed: 71.63 rpm synchronous speed, 90 rpm with SquareD, variable speed drive
- Cut-in wind speed: 6 m/s (some tests were run at 5 m/s)
- Power regulation: stall
- Rated power: 19.8 kW
- Tilt: 0°
- Cone angle: 0°, 3.4°, or 18°
- Location of rotor: upwind or downwind
- Rotational direction:
    - Downwind rotor: clockwise (viewed from downwind)
    - Upwind rotor: counter-clockwise (viewed from downwind)
- Rotor overhang: 1.469 m (yaw-axis to teeter pin).

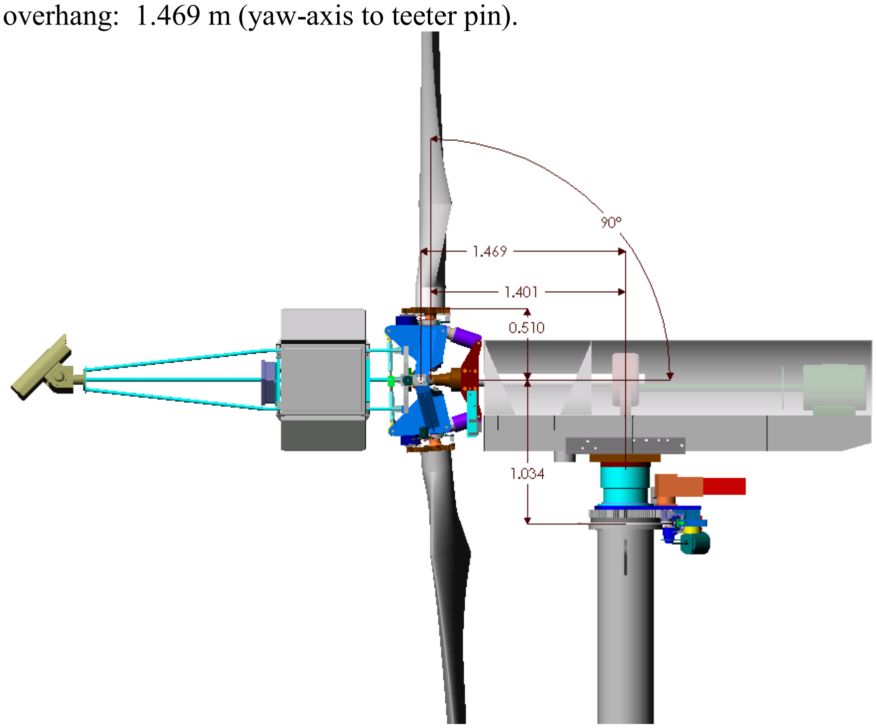

Figure A.1. Turbine rotor. (dimensions in meters).

Rotor

Geometry

- Blade cross-section and planform: NREL S809, tapered and twisted
- Root extension from center of rotation to airfoil transition: 0.883 m
- Blade tip pitch angle (manually set by turbine operator): 0°, 2°, 3°, 4°, 6°, cycling, ramping, (see each data file).

- Blade profile: NREL S809
- Blade chord: see Table A.1.
- Blade twist: see Table A.1.

Table A.1 Blade Chord and Twist Distributions

Radial Distance r (m)	Span Station[1] (r/5.532 m)	Span Station[1] (r/5.029 m)	Chord Length (m)	Twist[2] (degrees)	Thickness (m)	Twist Axis (% chord)
0.0	0.0	0.0	Hub - center of rotation	Hub - center of rotation	Hub – center of rotation	Hub - center of rotation
0.508[3]	0.092	0.101	0.218 (root hub adapter)	0.0 (root hub adapter)	0.218	50 (root hub adapter)
0.660[4]	0.120	0.131	0.218[5]	0.0	0.218	50
0.883	0.160	0.176	0.183[5]	0.0	0.183	50
1.008	0.183	0.200	0.349[5]	6.7	0.163	35.9
1.067	0.193	0.212	0.441[5]	9.9	0.154	33.5
1.133	0.205	0.225	0.544[5]	13.4	0.154	31.9
1.257	0.227	0.250	0.737[5]	20.040	0.154	30
1.343	0.243	0.267	0.728	18.074	20.95% chord	30
1.510	0.273	0.300	0.711	14.292	20.95% chord	30
1.648	0.298	0.328	0.697	11.909	20.95% chord	30
1.952	0.353	0.388	0.666	7.979	20.95% chord	30
2.257	0.408	0.449	0.636	5.308	20.95% chord	30
2.343	0.424	0.466	0.627	4.715	20.95% chord	30
2.562	0.463	0.509	0.605	3.425	20.95% chord	30
2.867	0.518	0.570	0.574	2.083	20.95% chord	30
3.172	0.573	0.631	0.543	1.150	20.95% chord	30
3.185	0.576	0.633	0.542	1.115	20.95% chord	30
3.476	0.628	0.691	0.512	0.494	20.95% chord	30
3.781	0.683	0.752	0.482	-0.015	20.95% chord	30
4.023	0.727	0.800	0.457	-0.381	20.95% chord	30
4.086	0.739	0.812	0.451	-0.475	20.95% chord	30
4.391	0.794	0.873	0.420	-0.920	20.95% chord	30
4.696	0.849	0.934	0.389	-1.352	20.95% chord	30
4.780	0.864	0.950	0.381	-1.469	20.95% chord	30
5.000	0.904	0.994	0.358	-1.775	20.95% chord	30
5.305	0.959	1.055	0.328	-2.191	20.95% chord	30
5.532	1.000	1.100	0.305	-2.500	20.95% chord	30

1) The blade radius is modified by changing the tip piece.
2) Twist convention is positive towards feather. Values listed are relative to zero twist at the 3.772 m station (75% span on a 5.029 m blade). Twist is 2.5 degrees toward stall at the tip.
3) Each blade attaches to the hub at a point 0.508 m from the center of rotation.
4) There is a cylindrical section at the root that extends from 0.508 m to 0.883 m. The airfoil transition begins at approximately the 0.883 m radial station.
5) There is a transition from the circular pitch shaft attachment to the S809 airfoil along the 0.883 m to 1.257 m region. The transition ends with a 0.737 m chord S809 airfoil at the 1.257 m span station.

- Airfoil distribution: Except for the root, the blade uses the S809 at all span locations. The airfoil coordinates are shown in Table A.2.

Table A.2. Airfoil Profile Coordinates

Upper Surface		Lower Surface	
x/c	**y/c**	**x/c**	**y/c**
0.00037	0.00275	0.00140	-0.00498
0.00575	0.01166	0.00933	-0.01272
0.01626	0.02133	0.02321	-0.02162
0.03158	0.03136	0.04223	-0.03144
0.05147	0.04143	0.06579	-0.04199
0.07568	0.05132	0.09325	-0.05301
0.10390	0.06082	0.12397	-0.06408
0.13580	0.06972	0.15752	-0.07467
0.17103	0.07786	0.19362	-0.08447
0.20920	0.08505	0.23175	-0.09326
0.24987	0.09113	0.27129	-0.10060
0.29259	0.09594	0.31188	-0.10589
0.33689	0.09933	0.35328	-0.10866
0.38223	0.10109	0.39541	-0.10842
0.42809	0.10101	0.43832	-0.10484
0.47384	0.09843	0.48234	-0.09756
0.52005	0.09237	0.52837	-0.08697
0.56801	0.08356	0.57663	-0.07442
0.61747	0.07379	0.62649	-0.06112
0.66718	0.06403	0.67710	-0.04792
0.71606	0.05462	0.72752	-0.03558
0.76314	0.04578	0.77668	-0.02466
0.80756	0.03761	0.82348	-0.01559
0.84854	0.03017	0.86677	-0.00859
0.88537	0.02335	0.90545	-0.00370
0.91763	0.01694	0.93852	-0.00075
0.94523	0.01101	0.96509	0.00054
0.96799	0.00600	0.98446	0.00065
0.98528	0.00245	0.99612	0.00024
0.99623	0.00054	1.00000	0.00000
1.00000	0.00000	0.00000	0.00000

(Butterfield et. al, 1992)

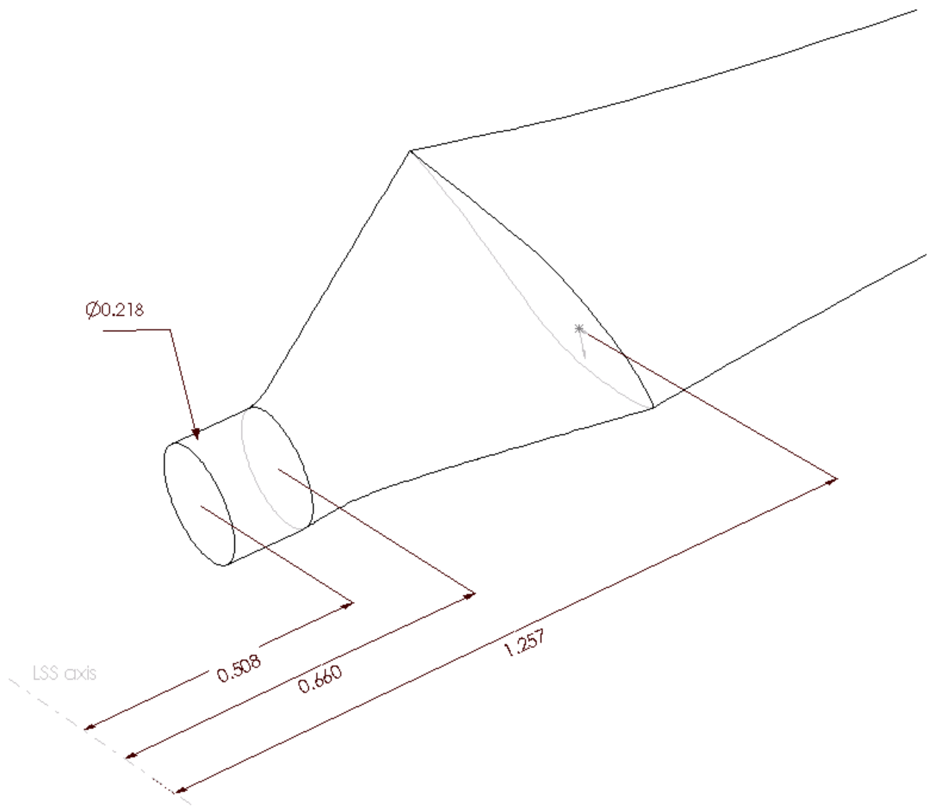

Figure A.2. Blade root surface depiction (dimensions in meters).

Aerodynamics for S809 Airfoil

- Aerodynamic coefficients (α = angle of attack; C_l = lift coefficient, C_{dp} = pressure drag coefficient) obtained at the Colorado State University wind tunnel with a Reynolds number of 300,000 are shown in Table A.3 (Butterfield et al. 1992).

Table A.3. Wind Tunnel Profile Coefficients from CSU

α	C_l	C_{dp}
0	0.105	0.0117
1.99	0.307	0.0116
4.08	0.545	0.0139
6.11	0.748	0.0135
8.14	0.88	0.0198
10.2	0.878	0.036
11.2	0.87	0.0446
12.2	0.854	0.0496
13.1	0.877	0.0619
14.1	0.894	0.0731
15.2	0.891	0.0865
16.3	0.745	0.22
17.2	0.591	0.248
18.1	0.592	0.265
19.2	0.58	0.279
20.2	0.604	0.298
22.1	0.588	0.323
26.2	0.669	0.412
30.2	0.946	0.633
35.2	1.02	0.799
40.3	1.08	0.983
45.2	1.23	1.31
45.1	1.13	1.21
50	1.21	1.51
60	1.05	1.86
69.9	0.805	2.27
80	0.456	2.16
90	0.128	2.24

- Aerodynamic coefficients (α = angle of attack; C_l = lift coefficient, C_{dp} = pressure drag coefficient) obtained at the Colorado State University wind tunnel with a Reynolds number of 500,000 are shown in Table A.4 (Butterfield et al. 1992).

Table A.4. Wind Tunnel Profile Coefficients from CSU

α	C_l	C_{dp}
-2.23	-6.00E-02	6.00E-03
-1.61E-01	1.56E-01	4.00E-03
1.84	3.69E-01	6.00E-03
3.88	5.71E-01	8.00E-03
5.89	7.55E-01	9.00E-03
7.89	8.60E-01	1.70E-02
8.95	8.87E-01	2.40E-02
9.91	8.69E-01	3.50E-02
10.9	8.68E-01	3.90E-02
12	8.94E-01	4.80E-02
12.9	9.38E-01	6.10E-02
14	9.29E-01	7.40E-02
14.9	9.08E-01	8.00E-02
16	9.12E-01	1.06E-01
17	6.55E-01	2.71E-01
18	5.88E-01	2.65E-01
19	5.87E-01	2.81E-01
20	5.97E-01	2.99E-01
22	6.03E-01	3.26E-01
24	6.47E-01	3.75E-01
26	6.83E-01	4.19E-01
28.1	7.45E-01	4.82E-01
30	8.24E-01	5.60E-01
35	1.05	8.17E-01
40	1.14	1.03
45	1.2	1.26
50	1.12	1.38
55	1.17	1.7
60	1.08	1.87
65	9.40E-01	1.98
70	8.57E-01	2.19
74.9	6.66E-01	2.17
79.9	4.72E-01	2.21
84.8	3.56E-01	2.32
89.9	1.42E-01	2.09

- Aerodynamic coefficients (α = angle of attack; C_l = lift coefficient, C_{dp} = pressure drag coefficient) obtained at the Colorado State University wind tunnel with a Reynolds number of 650,000 are shown in Table A.5 (Butterfield et al. 1992).

Table A.5. Wind Tunnel Profile Coefficients from CSU

α	C_l	C_{dp}
-0.25	0.151	0.002
1.75	0.354	0.001
3.81	0.561	0.002
5.92	0.765	0.006
7.94	0.86	0.015
9.98	0.848	0.031
11	0.892	0.043
12	0.888	0.049
13	0.927	0.043
14	0.91	0.075
15	0.91	0.075
16	0.928	0.107
17	0.686	0.278
18	0.639	0.276
19	0.576	0.273
20	0.552	0.275
22	0.596	0.323
23.9	0.649	0.37
26	0.68	0.417
30	0.851	0.576
35	1.01	0.789
40	1.12	1.03
45	1.12	1.19
50	1.1	1.36
55.3	1.08	1.58
60.2	0.931	1.62
65.2	0.968	2
70.2	0.776	2.04
75.2	0.63	2.13
80.2	0.485	2.32
85.1	0.289	2.14
90.2	0.109	2.27

- Aerodynamic coefficients (α = angle of attack; C_l = lift coefficient, C_{dp} = pressure drag coefficient; C_{dw} = total drag coefficient from wake traverse, C_m = moment coefficient) obtained at the Ohio State University wind tunnel with a Reynolds number from 730,000 to 770,000 are shown in Table A.6.

Table A.6. Wind Tunnel Profile Coefficients from OSU (Re=650,000)

α	C_l	C_{dp}	C_{dw}	C_m	Re x 10^6
-20.1	-0.56	0.3027		0.0612	0.76
-18.1	-0.67	0.3069		0.0904	0.75
-16.1	-0.79	0.1928		0.0293	0.75
-14.2	-0.84	0.0898		-0.009	0.75
-12.2	-0.7	0.0553		-0.0045	0.75
-10.1	-0.63	0.039		-0.0044	0.73
-8.2	-0.56	0.0233	0.0639	-0.0051	0.74
-6.1	-0.64	0.0112	0.0119	0.0018	0.74
-4.1	-0.42	-0.0004	0.0121	-0.0216	0.76
-2.1	-0.21	-0.0003	0.011	-0.0282	0.75
0.1	0.05	0.0029	0.0113	-0.0346	0.75
2	0.3	0.0056	0.0107	-0.0405	0.74
4.1	0.54	0.0067	0.0121	-0.0455	0.75
6.2	0.79	0.0085	0.0131	-0.0507	0.74
8.1	0.9	0.0127	0.0139	-0.0404	0.75
10.2	0.93	0.0274	0.0436	-0.0321	0.75
11.3	0.92	0.0303		-0.0281	0.74
12.1	0.95	0.0369		-0.0284	0.74
13.2	0.99	0.0509		-0.0322	0.74
14.2	1.01	0.0648		-0.0361	0.74
15.3	1.02	0.0776		-0.0363	0.74
16.3	1	0.0917		-0.0393	0.74
17.1	0.94	0.0994		-0.0398	0.73
18.1	0.85	0.2306		-0.0983	0.77
19.1	0.7	0.3142		-0.1242	0.76
20.1	0.66	0.3186		-0.1155	0.76
22	0.7	0.3694		-0.1265	0.76
24.1	0.79	0.4457		-0.1488	0.77
26.2	0.88	0.526		-0.1723	0.76

- Aerodynamic coefficients (α = angle of attack; C_l = lift coefficient, C_{dp} = pressure drag coefficient; C_{dw} = total drag coefficient from wake traverse, C_m = moment coefficient) obtained at the Ohio State University wind tunnel with a Reynolds number from 990,000 to 1,040,000 are shown in Table A.7.

Table A.7. Wind Tunnel Profile Coefficients from OSU (Re=1,000,000)

α	C_l	C_{dp}	C_{dw}	C_m	Re x 10^6
-20.1	-0.55	0.2983		0.0590	1.01
-18.2	-0.65	0.2955		0.0797	1.02
-16.2	-0.80	0.1826		0.0244	1.01
-14.1	-0.79	0.0793		0.0060	0.99
-12.1	-0.70	0.0547		-0.0043	1.01
-10.2	-0.63	0.0401	0.0750	-0.0035	1.00
-8.2	-0.58	0.0266		-0.0032	1.00
-6.2	-0.61	0.0183	0.0193	0.0088	1.00
-4.1	-0.40	0.0004	0.0127	-0.0245	0.99
-2.1	-0.16	0.0009	0.0090	-0.0308	1.00
0	0.07	0.0022	0.0085	-0.0356	1.01
2.1	0.30	0.0037	0.0088	-0.0394	1.00
4.1	0.55	0.0050	0.0088	-0.0461	1.00
6.1	0.79	0.0063	0.0090	-0.0499	1.00
8.2	0.90	0.0096	0.0167	-0.0364	1.00
10.1	0.94	0.0231	0.0487	-0.0396	1.00
11.2	0.93	0.0236		-0.0280	1.00
12.2	0.97	0.0368		-0.0307	1.00
13.3	1.00	0.0551		-0.0362	0.99
14.2	1.02	0.0618		-0.0365	0.99
15.2	1.03	0.0705		-0.0375	0.99
16.2	1.01	0.0880		-0.0430	1.00
17.2	0.95	0.1043		-0.0456	0.99
18.1	0.90	0.1325		-0.0581	1.00
19.2	0.78	0.3474		-0.1464	1.02
20	0.67	0.3211		-0.1171	1.02
22.1	0.70	0.3699		-0.1253	1.02
24	0.77	0.4348		-0.1430	1.03
26.1	0.91	0.5356		-0.1783	1.04

- Aerodynamic coefficients (α = angle of attack; C_l = lift coefficient, C_{dw} = total drag coefficient, C_m = moment coefficient) obtained at the Delft University of Technology Low Speed Laboratory low-turbulence wind tunnel with a Reynolds number of 1,000,000 are shown in Table A.8 (Somers 1997).

Table A.8. Wind Tunnel Profile Coefficients from DUT

α	C_l	C_{dw}	C_m
-1.04	0.019	0.0095	-0.0408
-0.01	0.139	0.0094	-0.0435
1.02	0.258	0.0096	-0.0462
2.05	0.378	0.0099	-0.0487
3.07	0.497	0.0100	-0.0514
4.10	0.617	0.0100	-0.0538
5.13	0.736	0.0097	-0.0560
6.16	0.851	0.0095	-0.0571
7.18	0.913	0.0127	-0.0506
8.20	0.952	0.0169	-0.0439
9.21	0.973	0.0247	-0.0374
10.20	0.952	0.0375	-0.0397
11.21	0.947	0.0725	-0.0345
12.23	1.007	0.0636	-0.0420
13.22	1.031	0.0703	-0.0420
14.23	1.055	0.0828	-0.0419
15.23	1.062	0.1081	-0.0418
16.22	1.043	0.1425	-0.0452
17.21	0.969	0.1853	-0.0458
18.19	0.938	0.1853	-0.0544
19.18	0.929	0.1853	-0.0658
20.16	0.923	0.1853	-0.0783

Structural Properties for 10.058 m diameter rotor, no 5-hole probes

- Rotor mass: 576.3 kg
- Pitch shaft, bull gear, instrumentation, bearings, nut, spacers: 38.6 kg (for one blade)
- Hub mass: 237.8 kg
- Boom, instrumentation enclosures, and camera mass: 141.9 kg
- Blade mass (without 5-hole probes but with probe plugs inserted):
  - Blade 1: Balanced to match Blade 3
  - Blade 3: 60.2 kg
  - Difference between 5-hole probe mounts and 5-hole probe plugs: 0.454 kg
  - Difference between smoke tip with smoke generator and regular tip: 1.089 kg (Blade 1 balanced with counter-weight)
- Blade center of gravity (from center of rotation):
  - Blade 1: Balanced to match Blade 3
  - Blade 3: 2.266 m
- Blade mass and stiffness distributions:
  - Estimates of mass and stiffness distributions were made by the blade manufacturer for the constant-chord, highly twisted blade used during Phase V testing (Composite Engineering 1994). The pressure instrumentation and counterweights were included, as well as the root mounted camera. The pitch shafts used during the wind tunnel test were also used for Phase V. There was no root-mounted camera during the wind tunnel test.

Table A.9. Phase V, Twisted Blade, Constant 0.457 m Chord, Structural Properties.

Distance from Rotor Center (m)	Mass (kg/m)	Flapwise Stiffness (Nm^2)	Edgewise Stiffness (Nm^2)
5.029	9.32	46953	365070
4.526	9.25	46953	387600
4.023	10.22	65974	436440
3.520	11.19	84468	512420
3.018	12.06	105560	583420
2.515	12.95	123480	650900
2.012	13.49	149420	737010
1.509	16.92	232180	997640
1.006	46.09	710230	1332800
0.749	45.18	1302400	1556800
0.508	30.14	2320700	2322100
0.402		473517	473517

  - Load is carried by a carbon fiber D-spar that tapers in thickness from root to tip. The carbon is primarily unidirectional with ±45° S-glass fibers interwoven. The D-spar in the tapered blade is larger at the root than that of the constant chord blade. Thus the tapered blade is substantially stiffer. The non-load carrying skin is fiberglass.

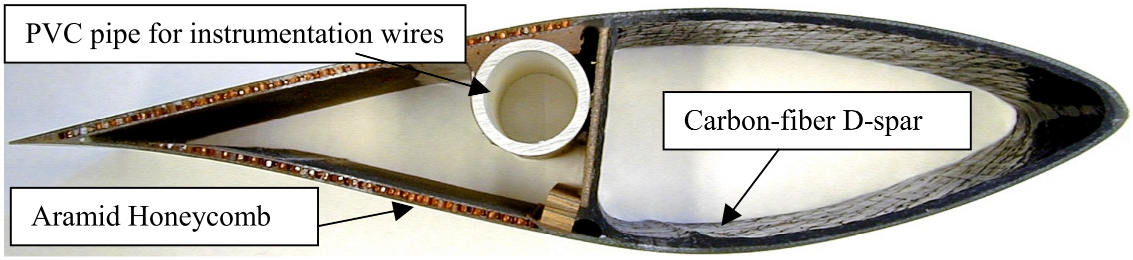

Figure A.3. Cross-section of blade.

- A modal test was performed with each blade attached to a pitch shaft that was clamped at the bearing locations. Figure A.4 illustrates the bearing locations and dimensions of the pitch shaft mount.

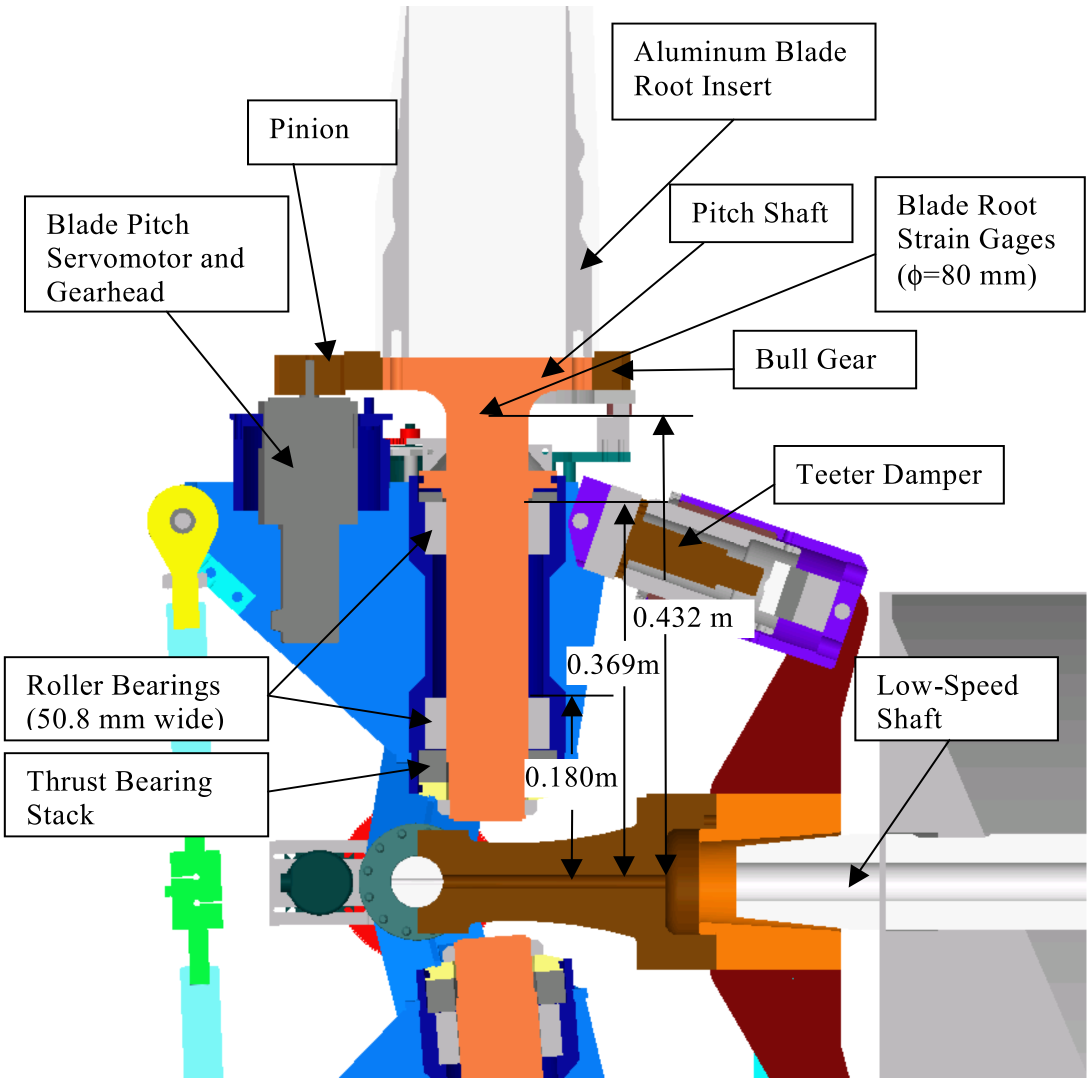

Figure A.4. Section view of pitch shaft mounted in hub.

Table A.10. Modal frequencies for both tapered and constant-chord blades

	Tapered, twisted blade	**Constant-chord, twisted blade**
First edgewise eigenfrequency		
Non-instrumented blade	9.062 Hz	8.16 Hz
Instrumented blade	8.9 Hz	7.97 Hz
First flapwise eigenfrequency		
Non-instrumented blade	7.313 Hz	4.94 Hz
Instrumented blade	7.25 Hz	4.79 Hz
Second flapwise eigenfrequency		
Non-instrumented blade	30.062 Hz	20.70 Hz
Instrumented blade	29.438 Hz	

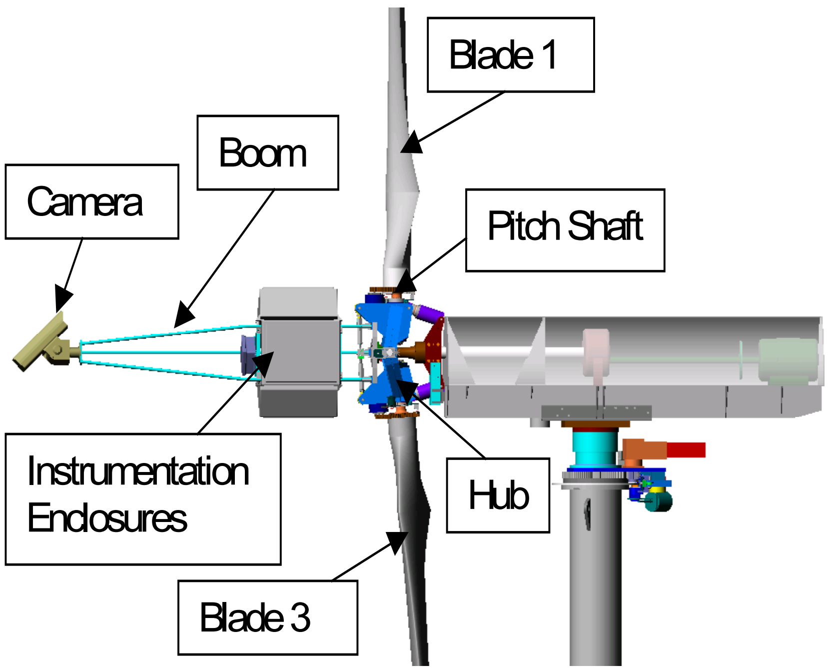

Figure A.5 Rotor Components.

Power Train

Layout

- The power train consists of the rotor mounted on a low-speed shaft coupled to a high-speed shaft via a gearbox. The high-speed shaft couples directly to an induction generator. The mechanical brake is positioned on the high-speed shaft.

Characteristics

- Rotor inertia: 949 kg m^2
- Inertia of rotating system (rotor, low-speed shaft, gearbox, high-speed shaft): 1093 kg m^2
- Power train inertia (low-speed shaft, gearbox, high-speed shaft, generator): 144-179 kg m^2
- Power train stiffness (low-speed shaft, gearbox, and high-speed shaft as a lumped parameter): $1.99 \cdot 10^5$ Nm/rad.
- Power train natural frequency: 5.78 Hz

- Power train damping: 0.06 to 0.08
- Gearbox ratio: 25.13:1
- Gearbox mounted on end of low-speed shaft. It is attached to the bedplate with a torque arm.
- High-speed shaft inertia: Not available
- High-speed shaft damping: 0.5% to 1.0%
- High-speed shaft stiffness: Not available
- Generator inertia: 143 kg m^2 w.r.t. low-speed shaft
- Generator slip: 1.69% at 20 kW
- Generator time constant: < 0.025 seconds (electro-mechanical time constant, for generator only)
- Power train efficiency:
  - Gearbox: 97% (from Grumman design documents)
  - Windage, couplings, main shaft bearings: 98% (from Grumman design documents)
  - Generator: The efficiency curve (in %) of the combined system (gearbox + generator) versus generator power (kW) is as follows:

    $$Eff = P_{gen}/((1.698641\cdot10^{-3})\cdot P_{gen}^{2} + (1.1270445\cdot10^{0})\cdot P_{gen} + (1.391369\cdot10^{0}))*100.$$

    Thus, the efficiency is fairly constant at about 78%.
- Maximum brake torque: 115 Nm

Power Train Computations

Rotor Inertia Computation

The inertia of the rotor itself was calculated using low-speed shaft torque and rate of change of rotor speed during startup of the turbine. The rotor was initially at rest. Then generator power was supplied initiating rotor rotation. Torque, azimuth angle, and generator power were recorded for 30 seconds. The data captured included initial ringing of the low-speed shaft as the rotation began. The data was processed with the MUNCH program which computed RPM from the rate of change of the azimuth angle.

The portion of the 30 second data file used in calculation of the rotor inertia was approximately one revolution of the instrumented blade in the region where the torque measurement was relatively constant. The sinusoidal correction for low-speed shaft torque was applied to the measured torque. The rotor speed at the endpoints of this region along with the average torque over this region provided the mass moment of inertia of the rotor about the low speed shaft as follows:

$$T = J\dot{\omega}$$

The test was performed two times, and the average inertia computed. All related charts are attached.

Table A.11. Rotor Inertia Computation

Test Name	dw/dt (rad/s^2)	Ave. Torque (Nm)	Standard Deviation	Rotor Inertia (kgm^2)
csstart1	2.34	-2210	81	946
csstart2	2.38	-2261	152	951
			Average:	949

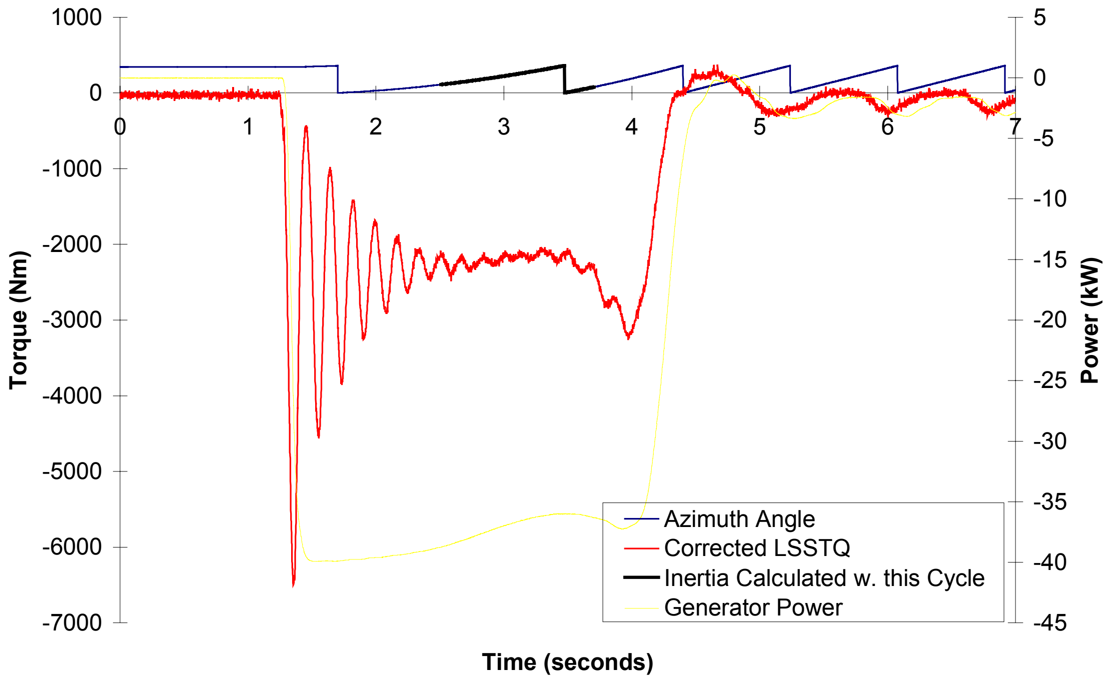

Figure A.6. Startup test csstart1.

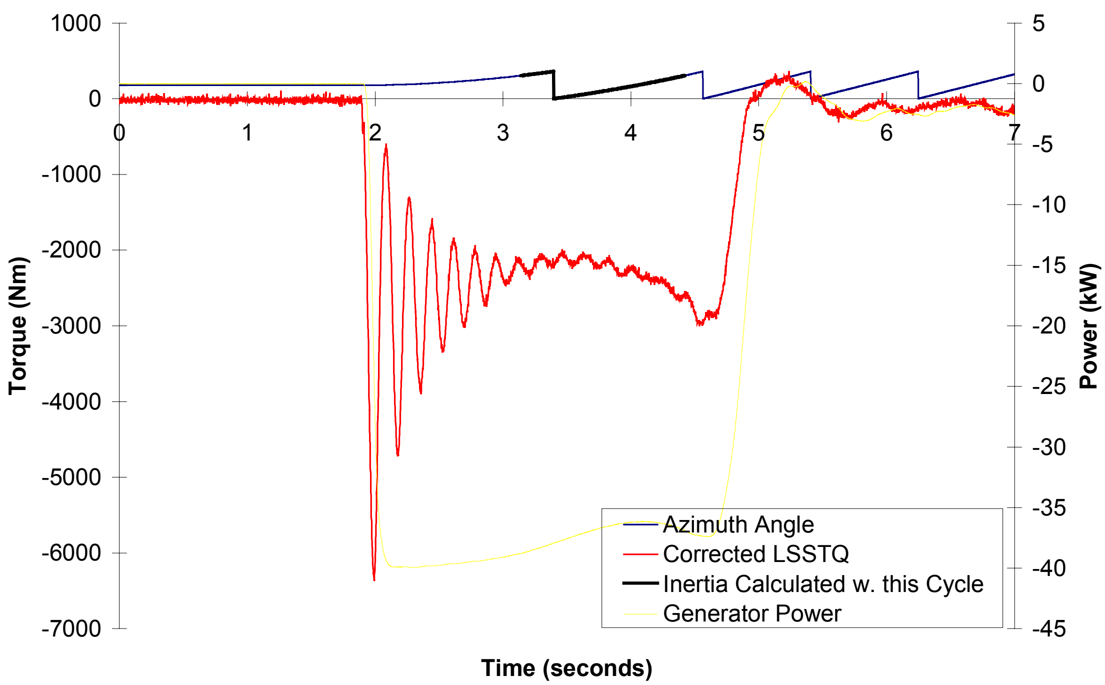

Figure A.7. Startup test csstart2.

Drive Train Inertia Computation

The inertia of the drive train was obtained by using the corrected low-speed shaft torque and rotational speed as the rotor slowed after disconnecting the generator power. Data was collected for 30 seconds while the rotor slowed. By pitching the blades toward feather after the generator is disconnected, the rotor speed decreases quickly reducing the effect of gearbox friction. Friction from the gearbox slows the rotor and causes the inertia to be under-estimated. The blades were pitched during one of the two stopping tests. The region with the fastest decrease in rotor speed over the shortest time was selected to compute the drive train inertia. The rotational speed change during the rotor slow-down and the corresponding average torque provided the mass moment of inertia of the drive train with respect to the low-speed shaft as follows:

$$T = J\dot{\omega}$$

Table A.12. Drive Train Inertia Computation

Test Name	dw/dt (rad/s^2)	Ave. Torque (Nm)	Standard Deviation	Drive Train Inertia (kgm^2)
csstop2	-1.98	-285	93	144

Due to the gearbox friction, this value underestimates the actual drive train inertia. During the Phase IV portion of testing, a pendulum test was performed on the three-blade turbine to determine the full-system inertia, and start-up tests were performed to determine the rotor inertia. The pendulum test consisted of placing a weight on the end of one blade and allowing the rotor to swing back and forth. The frequency of pendulum swings is used to compute the full system inertia. In this test, the gearbox friction reduces the frequency of oscillations which causes the inertia to be over-estimated. The difference between the rotor inertia obtained from start up tests and the full system inertia obtained from the pendulum test is the drive-train inertia, 179 kg m^2. The true drive train inertia should be bounded by these two tests.

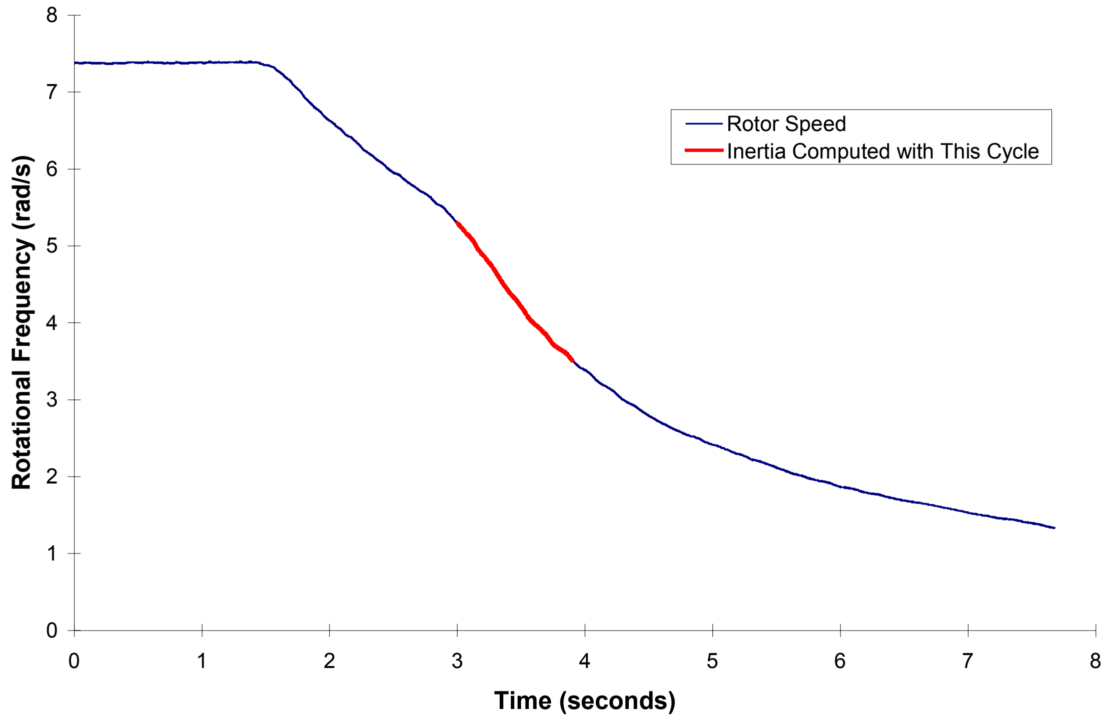

Figure A.8. Rotor speed decrease during stopping test csstop2.

Drive Train Damping and Frequency Computation

The startup tests were used to estimate the drive-train damping and natural frequency. As the generator power was initiated the torque measurement showed the drive-train dynamics. Determination of the damped frequency was made using the corrected torque measurement. The first cycle was neglected, but the time required for the next five complete cycles was calculated. The damped frequency was the quotient. The peaks for the torque cycles and the corresponding time was extracted from each of the startup tests. The mean of each half-cycle was computed and a polynomial curve fit as a function of time was determined. This mean torque was then subtracted from each of the peak values. The amplitude of successive peaks was used in the following formula to compute the damping:

$$\ln \frac{x_i}{x_{i+1}} \cong 2\pi\xi$$

The average and standard deviation of the first six consecutive pairs is shown in the table below. In addition, an exponential curve fit was applied to the mean-adjusted torque peaks. The damping and natural frequency values resulting from the equation solver are also included in the table.

Table A.13. Drive Train Damping and Damped Frequency

Test Name	Damping (measured)	Damping Standard Deviation	Damped Frequency, Hz (measured)	Damping (Exponential Curve Fit)	Natural Frequency, Hz (Exponential Curve Fit)
csstart1	0.07	0.01	5.70	0.06	5.70
csstart2	0.07	0.01	5.84	0.06	5.85
Average:	0.07	0.01	5.77	0.06	5.78

Drive Train Stiffness Computation

Knowledge of the rotor inertia and the generator inertia with respect to the low-speed shaft facilitate computation of the stiffness of all components in between if the natural frequency of these components is known. The stiffness of the low-speed shaft, gearbox, and high-speed shaft were thus determined:

$$K = \frac{(2 \pi f_n)^2}{\frac{1}{I_r} + \frac{1}{I_g}}$$

where I_r is the rotor inertia, I_g is the generator inertia, f_n is the measured natural frequency, and K is the stiffness of the lumped components between the rotor and the generator.

The natural frequency was computed from the measured damping and damped frequency resulting from the startup tests as follows:

$$\omega_d = \omega_n \sqrt{1 - \xi^2}$$

This was determined for both startup tests, and the stiffness was calculated using the corresponding rotor inertia determined for each test. The average stiffness was then calculated and is presented below:

Table A.14. Drive Train Natural Frequency and Stiffness

Test Name	Drive Train Natural Freq. (Hz)	Drive Train Stiffness (Nm/rad)
csstart1	5.71	1.94E+05
csstart2	5.85	2.04E+05
Average:	5.78	1.99E+05

Tower

Description

- Basic description: two different diameter cylinders connected by a short conical section. The conical section base is 3.4 m above the tower base. The conical section top is 3.9 m above the tower base. The base of the tower is a 1.829 m diameter flange that mounts to the semi-span mount below the floor of the wind tunnel. The wind tunnel floor is 0.356 m above the base of the tower.

Characteristics

- Tower material: ASTM A106 schedule 40 and schedule 80 Type B pipe, A36 ¾" plate
- Tower height: 11.5 m, 11.14 m above tunnel floor
- Tower diameter(base): 0.6096 m outer diameter, 0.0124 m inner diameter (design values)
- Tower diameter(top): 0.4064 m outer diameter, 0.0175 inner diameter (design values)
- Tower mass: 3317 kg
- Nacelle, hub, and boom mass: 1712 kg
- Position of tower head c.g.: Not available
- Nacelle, hub, and boom inertia: 3789 kg m^2
- First tower/nacelle eigenfrequency (x): 1.695 Hz
- Distance from top of tower flange to low-speed shaft: 1.034 m

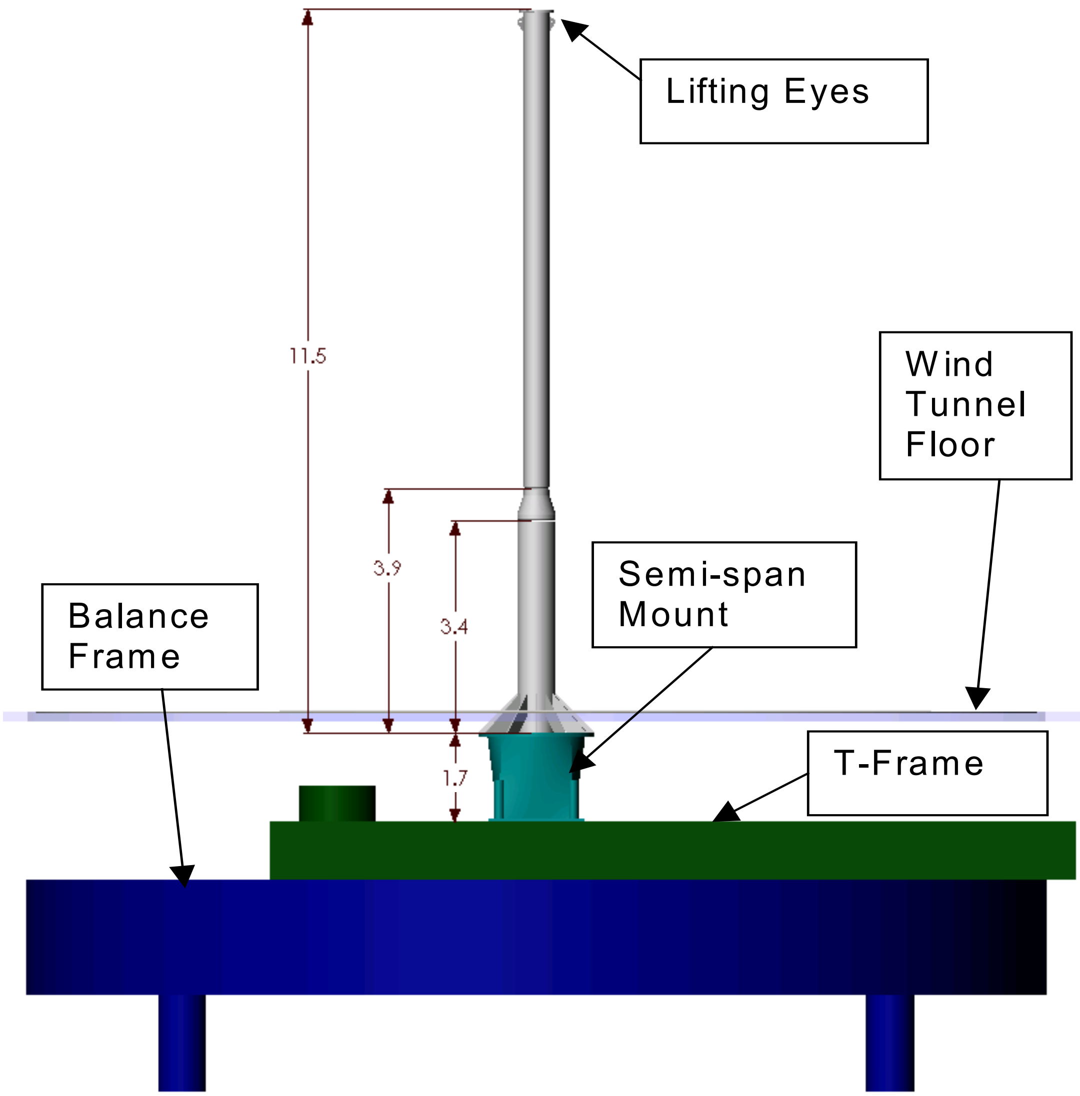

Figure A.9. Tower (dimensions in meters).

Modal Test Summary

Operational Turbine

Table A.15. Modes for turbine at 0° yaw and 90° azimuth.

Mode No.	Frequency [Hz.]	Damping [Hz.]	Damping %Cr
1	1.67	0.1	4.8
2	1.75	0.1	3.5
3	2.47	0.1	5.5
4	5.86	0.1	1.9
5	5.90	0.0	0.5
6	7.17	0.2	2.6
7	7.30	0.1	1.0
8	8.74	0.1	0.7
9	11.84	0.1	0.6
10	11.88	0.1	0.6
11	13.02	0.2	1.4
12	14.53	0.1	0.9
13	14.97	0.2	1.5
14	18.09	0.2	1.1
15	18.18	0.2	1.0
16	18.05	0.3	1.5
17	18.17	0.2	1.2
18	20.29	0.3	1.5
19	22.76	0.2	0.8
20	23.75	0.3	1.1
21	25.26	0.4	1.5

Turbine with blades removed

Table A.16. Modes for turbine with blades removed, instrumentation boxes installed.

Mode No.	Frequency [Hz.]	Damping [Hz.]	Damping %Cr
1	1.34	0.1	8.0
2	1.79	0.0	2.4
3	1.85	0.1	3.3
4	5.92	0.0	0.6
5	7.10	0.2	2.6
6	8.55	0.2	1.8
7	11.01	0.3	2.5
8	11.62	0.1	0.6
9	12.68	0.6	4.9
10	14.56	0.1	0.8
11	15.02	0.3	1.7
12	18.12	0.2	1.1
13	20.45	0.3	1.7
14	23.83	0.3	1.2
15	24.91	0.5	2.1

Tower alone

Table A.17. Modes for tower mounted to semi-span.

Mode No.	Frequency [Hz.]	Damping [Hz.]	Damping %Cr
1	1.74	0.1	6.3
2	2.36	0.2	6.5
3	2.73	0.1	3.2
4	3.91	0.0	0.5
5	4.03	0.0	0.6
6	8.14	0.1	1.2
7	10.38	0.2	2.0
8	10.66	0.2	1.6
9	11.93	0.1	0.5
10	14.01	0.3	2.2
11	14.75	0.1	0.6
12	18.07	0.3	1.8
13	19.50	0.2	0.9
14	19.91	0.1	0.7
15	21.03	0.1	0.3
16	22.04	0.3	1.3
17	24.80	0.2	1.0